The Interpath Relation for Spatially-Discrete Traveling-Wave Modulated Structures

Cody Scarborough, Anthony Grbic

Department of Electrical Engineering and Computer Science, University of Michigan,
Ann Arbor, Michigan, USA, e-mail: codyscar@umich.edu, agrbic@umich.edu

***Abstract*—Traveling-wave modulation has been employed since the 1950s for amplification and frequency conversion, and more recently for beam-steering and breaking reciprocity. Typically, traveling-wave modulation is realized by applying a staggered bias/pump signal to an array of discrete unit cells. This is referred to as spatially-discrete traveling-wave modulation (SD-TWM). SD-TWM structures can prove challenging to simulate due to their often complex geometry and extreme temporal variation. Here, we examine a relation established within SD-TWM structures referred to as the interpath relation. The interpath relation reveals that the solution within a single unit cell (as opposed to an entire spatial period) is sufficient to determine the entire problem. The interpath relation is then incorporated into a method of moments solver to compute the scattered field produced by a representative SD-TWM metasurface. The presented method simplifies the computation of both physical patterned designs, as well as nearly continuous idealized structures.**

***Index Terms*—Computational techniques, frequency-domain methods, interpath relation, metasurfaces, method of moments, N-path networks, periodic structures, space-time modulation, spatially-discrete traveling-wave modulation, traveling-wave modulation.**

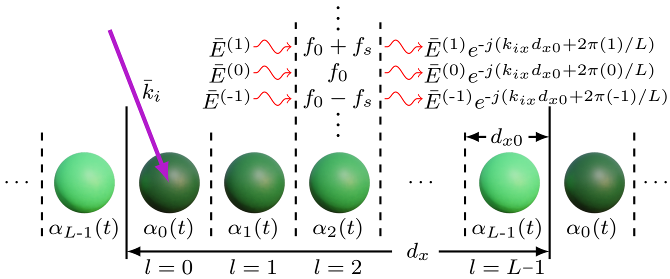

Fig. 1: Spatially-discrete traveling-wave modulation of an infinite array of scatterers. The structure is periodic in time with period T_s. Each supercell (solid borders) has a width of d_x while each stixel (dashed borders) has a width of $d_{x0} = d_x/L$. The time-varying parameter (e.g. polarizability) in stixel l is related to stixel $l-1$ as $\alpha_l(t) = \alpha_{l-1}(t - T_s/L)$. When illuminated by a plane wave, the frequency harmonics of the field at the boundaries of a stixel are related as shown.

I. Introduction

Traveling-wave modulation is a particular form of space-time modulation that has been shown to enable amplification, frequency-conversion, beam-steering, and non-reciprocity [1]–[5]. Research interest in traveling-wave modulation has been renewed due to improvements in the performance of tunable elements such as varactor diodes [1], phase-change materials [5]–[7] and electro-/magneto-optic materials [2], [7]; in addition to recent demonstrations of its ability to break reciprocity [2]–[4]. Typically, traveling-wave modulation is analyzed in the continuous limit, i.e. the modulated parameter is a continuous function of both space and time. In this case, the modulated parameter can be expressed in the form $f(t - xT_s/d_x)$ where T_s is the temporal period of the modulation and d_x is the spatial period. This form of modulation has been applied since the 1950s to achieve both frequency conversion and amplification [8]. Since then, the applications of traveling-wave modulation have expanded to include beam-steering and non-reciprocity [2]–[4].

Recent physical realizations of traveling-wave modulated structures often consist of a spatially discrete array of unit cells as shown in Fig. 1 [1]–[3], [7]. We refer to this form of modulation as spatially-discrete traveling-wave modulation (SD-TWM). Each spatial period, or supercell, contains a number, L, of smaller elements, referred to as stixels (space-time pixels). If the spatial period is d_x, then the width of each stixel is $d_{x0} = d_x/L$. The time dependence within stixel l is delayed with respect to stixel $l-1$ by T_s/L. As a result, the modulated parameter in any given stixel can be written $f(t - lT_s/L)$, which is simply the spatially-discrete form of $f(t - xT_s/d_x)$. In addition to mimicking continuous traveling-wave modulation, SD-TWM has been used recently to enable unique electromagnetic effects, such as subharmonic mixing, which cannot arise in the continuous limit [1].

Complex unit cell geometries and extreme temporal variation can make SD-TWM structures difficult to simulate to sufficient accuracy. Numerical methods reported to date capable of analyzing these structures require the computational domain to extend over an entire supercell [9]–[12]. In this presentation, we exploit a boundary condition established within SD-TWM structures, referred to as the interpath relation [13]. Using the interpath relation, it can be shown that the fields within a single stixel are sufficient to determine the entire problem. Here, the interpath relation is applied to the method of moments (MOM) to dramatically reduce computational complexity. In particular, numerical results for the SD-TWM structure presented in [1] are reported. The interpath relation dramatically reduces the computational cost of simulating SD-TWM structures

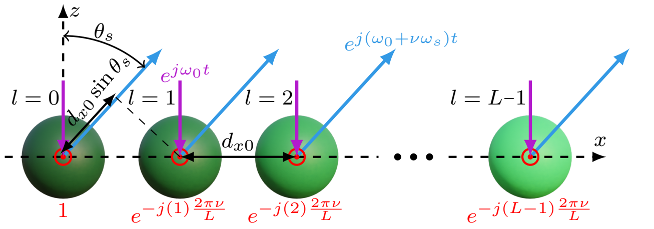

Fig. 2: Array interpetation of the scattering due to a single supercell of a SD-TWM structure assuming a normally incident excitation. The incident wave (dark purple) is at a frequency f_0, while the observed frequency (light blue) can be any harmonic $f_0 + \nu f_s$. The relative phase induced within each stixel corresponding to observed frequency $f_0 + \nu f_s$ is shown in red below the scatterers.

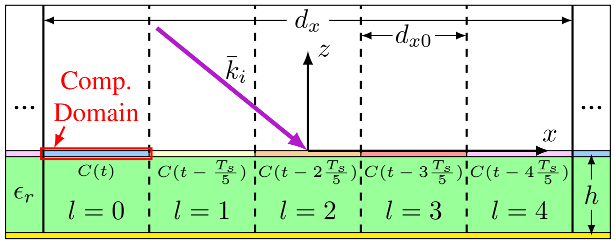

Fig. 3: SD-TWM structure proposed in [1] which consists of a SD-TWM capacitive sheet placed above a grounded dielectric. In this example, there are 5 stixels included within each supercell. The capacitance within stixel l is delayed with respect to stixel $l-1$ by $T_s/L = T_s/5$. Using the interpath relation, the computational domain can be reduced to the capacitive sheet within a single stixel (outlined in red).

such that researchers can carry out full-wave optimizations of patterned unit cells. The presented technique can also be used to greatly simplify the simulation of continuous traveling-wave modulated structures by sufficiently reducing the stixel size.

II. The Interpath Relation for Spatially-Discrete Traveling-Wave Modulation

In this section, we will examine and interpret the interpath relation derived in [13] for SD-TWM structures. Consider a SD-TWM structure, like the one in Fig. 1, illuminated by a plane wave at frequency f_0. In this case, SD-TWM is applied along x. The supercell size is assumed to be d_x, and there are L stixels per supercell. Since the system is linear and periodically time-varying, the field throughout space can be expanded into frequency harmonics as [14]

$$\bar{\mathcal{E}}(x,t) = \sum_{\nu=-\infty}^{\infty} \bar{E}^{(\nu)}(x)\, e^{j(\omega_0+\nu\omega_s)t}. \tag{1}$$

It was shown in [13], that when a SD-TWM structure is illuminated by a monochromatic plane wave, the frequency harmonics (ν) in the expansion above satisfy

$$\bar{E}^{(\nu)}(x) = e^{-j(k_{ix}d_{x0}+2\pi\nu/L)}\bar{E}^{(\nu)}(x-d_{x0}), \tag{2}$$

where $d_{x0} = d_x/L$ is the stixel dimension. The expression in (2) is the interpath relation and states that field harmonics separated by a stixel dimension are related by a frequency dependent phase delay.

The interpath relation in (2) provides physical insight into the scattering behavior of SD-TWM structures. This can be seen by examining the array factor produced by a single supercell. For simplicity, let us assume that the excitation is normally incident ($k_{ix} = 0$) as shown in Fig. 2. From (2), we observe that the relative phase of the induced fields within stixel l for frequency $f_0 + \nu f_s$ is $-2\pi l\nu/L$. Thus the array factor can be written

$$\mathrm{AF}(\theta) = \sum_{l=0}^{L-1} e^{jl\left(\frac{\omega_0+\nu\omega_s}{c}d_{x0}\sin\theta_s - \frac{2\pi\nu}{L}\right)}, \tag{3}$$

where θ_s is the angle of observation. From this expression, standard array theory [15] can be used to show that the beam-pointing angle(s) for a given frequency $f_0 + \nu f_s$ satisfies

$$\frac{\omega_0+\nu\omega_s}{c}d_{x0}\sin\theta_s = \frac{2\pi\nu}{L} + 2\pi p, \tag{4}$$

where $\lambda_0 = c/f_0$ and p is an integer. The beam-pointing expression in (4) reveals several interesting features of SD-TWM structures. Suppose the modulation frequency is much smaller than the excitation frequency ($f_s \ll f_0$). In this case, when ν is replaced by $\nu + L$, the beam-pointing angle(s) remains the same (since we are free to choose p). For example, the beam-pointing angle corresponding to f_0 ($\nu = 0$) would be the same as $f_0 + nLf_s$ for any integer n. This can be exploited to achieve subharmonic mixing: where the reflected wave is frequency converted by an integer multiple of the modulation frequency. Further, when d_{x0} is sufficiently subwavelength, it can be seen from (4) that there may be some frequencies which do not correspond to real values of θ_s. These frequencies are bound to the near-field of the structure.

III. The Interpath Relation within the Method of Moments

The interpath relation can be incorporated into a numerical simulator as a frequency harmonic dependent periodic boundary condition to reduce the computational domain. A standard computational method for analyzing a SD-TWM structure would require periodic boundaries to be placed at the boundaries of a supercell. Therefore, by enforcing the interpath relation at the boundaries of a single stixel, the number of required unknowns is reduced by a factor of L, the number of stixels per supercell. This can be done for arbitrarily small stixel sizes, which implies that the interpath relation can also be used to analyze nearly continuous structures. Without the interpath relation, a continuous structure would still have to be discretized into individual time-varying cells (effectively stixels) over an entire spatial period. Thus, when the interpath relation is applied to these cases, the domain contains only a single computational element.

As an example, let us apply the interpath relation in computing the scattered field produced by the structure shown in Fig. 3 [1]. The structure in Fig. 3 consists of a SD-TWM capacitive sheet placed above a grounded dielectric. The illuminating plane wave is assumed to be at 10 GHz and incident at an angle of 25°. The dielectric has a permittivity of $\epsilon_r = 3.55$ and thickness $h = 508$ μm. Each stixel has a width of $d_{x0} = 3$ mm and there are $L = 5$ stixels included per supercell. The boundary condition imposed by the impedance sheet is

$$\bar{\mathcal{J}}\left(x,t\right) = \frac{\partial}{\partial t}\left\{C\left(x,t\right)\bar{\mathcal{E}}_t\left(x,t\right)\right\}, \tag{5}$$

where $\bar{\mathcal{E}}_t$ is the component of time-dependent electric field in the x-y plane. To obtain the standard method of moments formulation for such a structure, the current would be expanded into spatio-temporal basis functions. Let us assume the following expansion for the current [16]

$$\bar{\mathcal{J}}\left(x,t\right) = e^{j(\omega_0 t - k_{ix}x)}\sum_{\nu=-U'}^{U'}\sum_{m=1}^{LM} e^{j\nu\omega_s t}\overleftrightarrow{W}_m\left(x\right)\bar{j}_m^{(\nu)}, \tag{6}$$

where

- U' is an integer which truncates the frequency spectrum
- M is the number of spatial samples in a single stixel
- $\overleftrightarrow{W}_m$ is a suitable spatial basis function [16] which satisfies $\overleftrightarrow{W}_m(x) = \overleftrightarrow{W}_{m-M}(x - d_{x0})$.

The expansion in (6) does not utilize the interpath relation. As a result, the total number of unknowns is $(2U'+1)ML$. However, by substituting (6) into the interpath relation in (2), we conclude $\bar{j}_m^{(\nu)} = e^{-j2\pi\nu/L}\bar{j}_{m-M}^{(\nu)}$. This allows us to rewrite (6) in terms of the unknowns within a single stixel (outlined in red in Fig. 3):

$$\bar{\mathcal{J}}\left(x,t\right) = e^{j(\omega_0 t - k_{ix}x)}\sum_{\nu=-U'}^{U'}\sum_{m=1}^{M} e^{j\nu\omega_s t}\overleftrightarrow{B}_m\left(x\right)\bar{j}_m^{(\nu)}, \tag{7}$$

where

$$\overleftrightarrow{B}_m\left(x\right) = \sum_{l=0}^{L-1} e^{-j2\pi\nu l/L}\overleftrightarrow{W}_m\left(x - l d_{x0}\right). \tag{8}$$

Note that the spatial summation in (7) is bounded by M rather than LM as in (6). This reduces the number of unknowns by a factor of L, the number of stixels per supercell. The modified basis function $\overleftrightarrow{B}_m$ simply applies the appropriate phase from the interpath relation to current within each stixel.

The modified MOM formulation was benchmarked against a spectral domain method reported in [1]. When the time-dependence of the capacitance within each stixel follows a tangent function, it can be shown [1] that the structure in Fig. 3 will upconvert the reflected wave to the fifth harmonic. This behavior is confirmed by examining the normal power scattered from the structure for each frequency harmonic as shown in Fig. 4. It can be seen that the two methods are in good agreement.

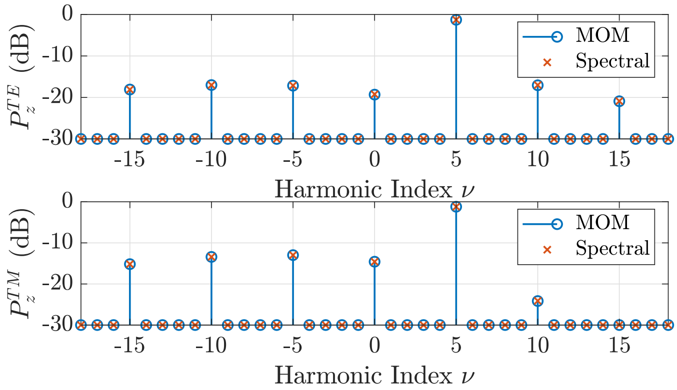

Fig. 4: Normal power radiated at each frequency $f_0 + \nu f_s$ from the metasurface in Fig. 3 [1]. In this configuration, the metasurface up-converts the scattered field to the fifth harmonic. It can be seen that the MOM solver and spectral domain method are in good agreement.

IV. Conclusion

The interpath relation is critical to the understanding and analysis of spatially-discrete traveling-wave modulated (SD-TWM) structures. Applying standard array theory to the interpath relation provides valuable insight into the scattering behavior of SD-TWM structures. This theory is capable of predicting unique electromagnetic phenomena, such as subharmonic mixing, which do not arise from the continuous model of traveling-wave modulation. From a practical viewpoint, the interpath relation reveals that the fields within a single stixel are sufficient to determine the fields in all space. This reduces the number of unknowns required in the numerical simulation of SD-TWM structures by a factor of L, the number of stixels per supercell. Such a reduction will allow researchers to efficiently carry out accurate full-wave optimizations of patterned SD-TWM structures prior to fabrication. Further, the interpath relation can be used to dramatically reduce the computational cost of numerically simulating continuous traveling-wave modulated structures.

Acknowledgment

This work was supported under the AFOSR MURI program FA9550-18-1-0379.

References

[1] Z. Wu, C. Scarborough, and A. Grbic, "Theoretical and experimental investigations of spatio-temporally modulated metasurfaces with spatial discretization," *arXiv:2006.06394*, June 2020.

[2] M. M. Salary, S. Jafar-Zanjani, and H. Mosallaei, "Nonreciprocal optical links based on time-modulated nanoantenna arrays: Full-duplex communication," *Phys. Rev. B*, vol. 99, p. 045416, Jan 2019. [Online]. Available: https://link.aps.org/doi/10.1103/PhysRevB.99.045416

[3] A. E. Cardin, S. R. Silva, S. R. Vardeny, W. J. Padilla, A. Saxena, A. J. Taylor, W. J. Kort-Kamp, H.-T. Chen, D. A. Dalvit, and A. K. Azad, "Surface-wave-assisted nonreciprocity in spatio-temporally modulated metasurfaces," *Nature communications*, vol. 11, no. 1, pp. 1–9, 2020.

[4] Y. Mazor and A. Alu, "One-way hyperbolic metasurfaces based on synthetic motion," *IEEE Transactions on Antennas and Propagation*, vol. 68, no. 3, pp. 1739–1747, 2020.

[5] Q. Wang, E. T. Rogers, B. Gholipour, C.-M. Wang, G. Yuan, J. Teng, and N. I. Zheludev, “Optically reconfigurable metasurfaces and photonic devices based on phase change materials,” *Nature Photonics*, vol. 10, no. 1, pp. 60–65, 2016.

[6] T. G. Folland, A. Fali, S. T. White, J. R. Matson, S. Liu, N. A. Aghamiri, J. H. Edgar, R. F. Haglund, Y. Abate, and J. D. Caldwell, “Reconfigurable infrared hyperbolic metasurfaces using phase change materials,” *Nature communications*, vol. 9, no. 1, pp. 1–7, 2018.

[7] A. M. Shaltout, V. M. Shalaev, and M. L. Brongersma, “Spatiotemporal light control with active metasurfaces,” *Science*, vol. 364, no. 6441, 2019.

[8] P. Tien and H. Suhl, “A traveling-wave ferromagnetic amplifier,” *Proceedings of the IRE*, vol. 46, no. 4, pp. 700–706, 1958.

[9] S. A. Stewart, T. J. Smy, and S. Gupta, “Finite-difference time-domain modeling of space–time-modulated metasurfaces,” *IEEE Transactions on Antennas and Propagation*, vol. 66, no. 1, pp. 281–292, 2018.

[10] Y. Vahabzadeh, N. Chamanara, K. Achouri, and C. Caloz, “Computational analysis of metasurfaces,” *IEEE Journal on Multiscale and Multiphysics Computational Techniques*, vol. 3, pp. 37–49, 2018.

[11] S. Taravati and G. V. Eleftheriades, “Generalized space-time-periodic diffraction gratings: Theory and applications,” *Phys. Rev. Applied*, vol. 12, p. 024026, Aug 2019. [Online]. Available: https://link.aps.org/doi/10.1103/PhysRevApplied.12.024026

[12] Y. Hadad, D. L. Sounas, and A. Alu, “Space-time gradient metasurfaces,” *Phys. Rev. B*, vol. 92, p. 100304, Sep 2015. [Online]. Available: https://link.aps.org/doi/10.1103/PhysRevB.92.100304

[13] C. Scarborough and A. Grbic, “Modified floquet boundary condition for open boundary problems with n-path symmetry,” in *2020 14th International Congress on Artificial Materials for Novel Wave Phenomena (Metamaterials)*, 2020.

[14] J. A. Richards, *Analysis of Periodically Time Varying Systems*. New York, NY: Springer-Verlag, 1983.

[15] C. A. Balanis, *Antenna Theory Anlysis and Design*. Hoboken, New Jersey: John Wiley & Sons, Inc., 2016.

[16] J.-M. Jin, *Theory and computation of electromagnetic fields*. John Wiley & Sons, 2011.